Front. Earth Sci. 2015, 9(3): 521–530
DOI 10.1007/s11707-015-0493-8

RESEARCH ARTICLE

A new method for recovering paleoporosity of sandstone: case study of middle Es3 member of Paleogene formation in Niuzhuang Sag, Dongying Depression, Bohai Bay Basin in China

Mingjie LIU (✉)[1], Zhen LIU[2], Biao WANG[3], Xiaoming SUN[2], Jigang GUO[4]

1 School of Geoscience and Technology, Southwest Petroleum University, Chengdu 610500, China
2 State Key Laboratory of Petroleum Resources and Prospecting, China University of Petroleum (Beijing), Beijing 102249, China
3 The Huabei Oilfield Company of PetroChina, Cangzhou 061023, China
4 Strategic Research Center of Oil and Gas Resources, Ministry of Land and Resources, Beijing 100034, China

Abstract This paper presents a new method for recovering paleoporosity of sandstone reservoirs and quantitatively defines the evolution process of porosity. This method is based on the principle that the present is the key to the past. We take the middle Es3 member in Niuzhuang Sag, Dongying Depression, and Bohai Bay Basin as an example. The method used in this study considers the present porosity as a constraint condition, and the influences of both constructive diagenesis and destructive diagenesis to divide the porosity evolution process into two independent processes, namely porosity increase and porosity decrease. An evolution model of sandstone porosity can be established by combining both the pore increase and pore decrease effects. Our study reveals that the porosity decrease model is a continuous function of burial depth and burial time, whereas the porosity increase model mainly occurs in an acidified window for paleotemperature of 70°C to 90°C. The porosity evolution process can be divided into the following phases: normal compaction, acidification and pore increase, and post-acidification compaction. Thus, the porosity evolution model becomes a piecewise function of three subsections. Examples show that the method can be applied effectively in recovering the paleoporosity of sandstone reservoirs and simulating the porosity evolution process.

Keywords paleoporosity, binary function, acidified window, Niuzhuang Sag, Bohai Bay Basin

Received December 11, 2013; accepted August 18, 2014

E-mail: liumingjieldd@163.com

1 Introduction

One of the main issues in geology is the recovery of sandstone paleoporosity. This study explains the evolution process of sandstone reservoir porosity in different historic stages. Research on the recovery of sandstone paleoporosity is significant for both theoretical study and practical application. Results can help to quantitatively recover paleoporosity conditions and process of accumulation.

Several authors have attempted to recover sandstone paleoporosity (Wangen, 1998; He et al., 2002; Dillon et al., 2004; Zhu et al., 2012) and have provided methods from the following aspects. 1) The principle that the present is the key to the past is applied, and the relation between present porosity of sandstone and burial depth is established to obtain paleoporosity if ancient burial depth is determined via burial history analysis (Deng et al., 2009). This method ignores the diagenesis and the effect of other factors at the same burial depth. Thus, accurately recovering the paleoporosity of sandstone characterized by old age and deep burial depth is difficult. 2) Calculating the effects of various forms of diagenesis on porosity evolution based on thin section observations combined with the diagenetic sequence can modify the apparent porosity in different phases (Li et al., 2009; Wang et al., 2011; Yang et al., 2012). This method requires observing massive numbers of thin sections and quantifying the diagenetic sequence. This method can recover paleoporosity only in the key diagenesis stage, so operability and practicality of this method should be improved. 3) A diagenesis index is proposed by combining the characteristics of the modern porosity profile, a diagenesis stage analysis, and thin section observations. A model of the diagenesis index and porosity is established to predict the porosity of a sandstone reservoir before drilling (Bloch et al., 1990; 2002; Bloch and Helmold, 1995; Meng et al., 2007). However, this method lacks porosity simulation and does not fully consider the influence of constructive diagenesis. The accuracy of paleoporosity recovery should be improved. 4) A comprehensive impact factor is proposed by considering the controlling factors for the porosity of the sandstone reservoir in different stages of diagenesis (Qu et al., 2012). Real data are used to illustrate porosity evolution under various impact factors. These factors contribute to the restoration of paleoporosity retained during the accumulation period. This method is an improvement of the method stated in 1). However, the restoration of paleoporosity is limited to the key accumulation period. Thus, this technique needs further improvement.

Sandstone porosity evolves with the diagenesis of strata (Ehrenberg, 1990; Pan et al., 2011). Based on previous methods, an effect simulation method is proposed in the present study. More specifically, the method simulates superposition effects after diagenesis through geological parameters instead of simulating diagenesis. Based on characteristics of modern porosity profiles and principles of effect-oriented simulation, the evolution of sandstone porosity is decomposed into porosity decrease and porosity increase processes. The porosity decrease process mainly involves compaction and cementation, while the porosity increase process mainly involves dissolution. The combination of these two independent processes forms the evolution of sandstone porosity.

2 Geologic setting and stratigraphy

Bohai Bay Basin, an important hydrocarbon-producing basin in China, is located in the eastern part of the country and covers an area of approximately 200,000 km^2. Since the Paleogene period, this basin has undergone a complex tectonic evolution which can be divided into the synrift stage and the postrift stage (Hu et al., 2001). The Bohai Bay Basin consists of several subbasins, namely, Liaohe, Liaodong Bay, Bozhong, Jiyang, Huanghua, Jizhong, and Linqing, as shown in Fig. 1(a) (Gong, 1997).

The Dongying Depression lies south of the Jiyang Subbasin and has an area of 5,850 km^2 (Zhang et al., 2009). Four sags (Minfeng, Lijin, Niuzhuang, and Boxin) further divide the Dongying Depression by several normal faults and an uplift in the central anticline belt (Fig. 1(b)). The Dongying Depression is an asymmetric “dustpan-shaped” lacustrine basin that developed as a result of a tertiary rift. Figure 1(c) shows that the depression is formed by five secondary tectonic zones from north to south, namely, northern steep slope zone, northern zone (Lijin Sag), central anticline zone, southern zone (Niuzhuang Sag), and southern gentle slope zone (Guo et al., 2010).

The depression is filled with Cenozoic sediments which are composed of formations from the Paleogene, Neogene, and Quaternary periods. Figure 2 shows that the formations from the Paleogene period are Kongdian (Ek), Shahejie (Es), and Dongying (Ed). The formations from the Neogene period are Guantao (Ng) and Minghuazhen (Nm). The formation from the Quaternary period is Pingyuan (Qp). Several authors have provided detailed descriptions of Paleogene stratigraphy (Zhang et al., 2004; Guo et al., 2012). The most important petroleum generation and accumulation layer, Es, can be divided into four members, Es1 through Es4, where Es1 is youngest and Es4 is oldest. Es3 has a thickness ranging from 700 m to 1,200 m and is characterized by lacustrine oil shale with high sedimentation rates, dark gray mudstones, and calcareous mudstones. Es3 can be further divided into three members, namely, upper Es3, middle Es3, and lower Es3, where upper Es3 is youngest and lower Es3 is oldest (Lampe et al., 2012).

The Niuzhuang Sag, which is located southeast of the Dongying Depression, covers 600 km^2. This area is oriented largely east to west. This sag has simple tectonic features composed primarily of synclines. Few faults exist in this area, except at the boundaries of the rift basin. Strata generally develop completely in the Niuzhuang Sag. This study mainly focuses on the western part of the Niuzhuang Sag and middle Es3 member. When the target stratum was deposited, the tectonic movement was strong and the basin diminished rapidly. Therefore, large amounts of detrital materials were transported into the basin and formed sedimentary facies of delta and turbidite fans (Li, 2004; Chen et al., 2009).

3 Method

3.1 Paleoporosity recovery principle

The focus of this study is the recovery of paleoporosity during the accumulation period, which is determined by applying the principle of effect-oriented simulation. According to the porosity variation effect, the porosity evolution process can be divided into an increasing pore model and a decreasing pore model (Fig. 3). Actual porosity in geological history is determined when both models are superimposed at the same point in geologic time or at the same burial depth.

3.2 Decreasing pore model

Compaction and cementation affect the decreasing poros-

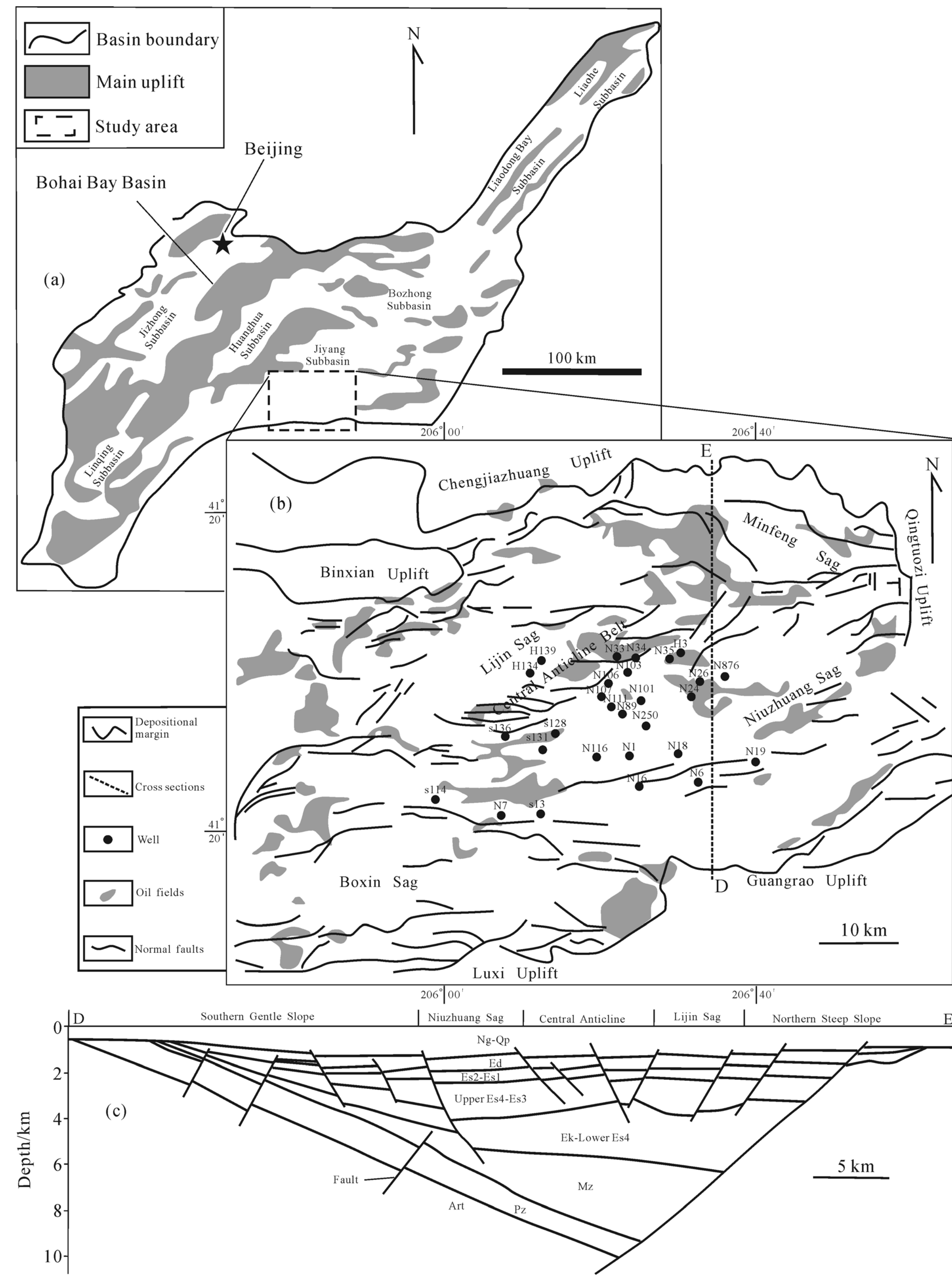

Fig. 1 (a) Location map showing the six major subbasins of the Bohai Bay Basin. (b) Map inset showing the oil field distribution, the locations of sections DE and FG, wells, and the normal faults for the top of the Es3 layer in the study area. (c) Cross section DE showing the different tectonic-structural zones and key stratigraphic intervals.

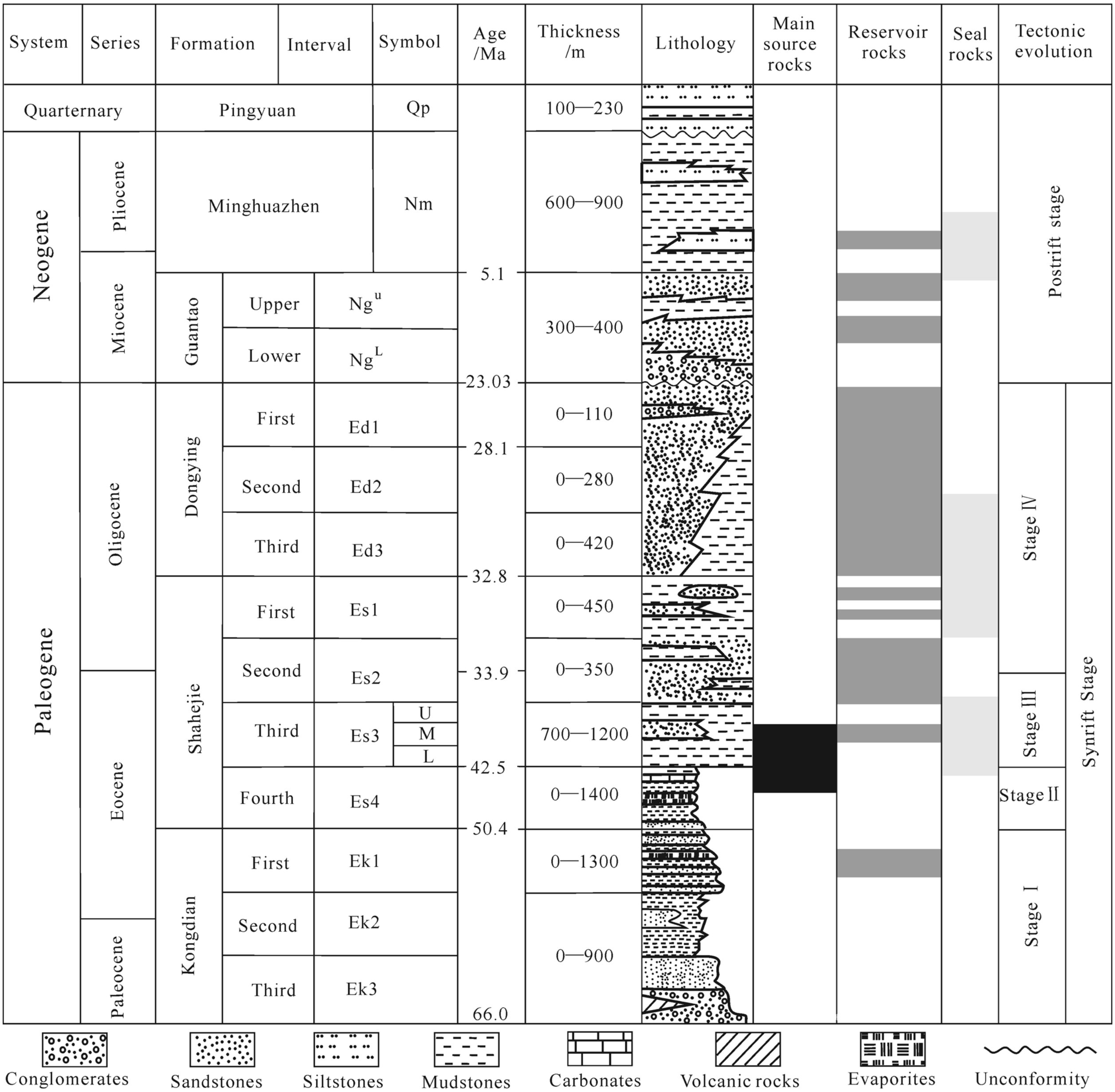

Fig. 2 Schematic of the Cenozoic-Quaternary stratigraphy of the Niuzhuang Sag showing the tectonic evolution stages and the major petroleum system elements.

ity of the middle Es3 member. In addition, the effect of decreasing pores is continuous with the burial of strata. Compaction plays a major role in this process, particularly in the shallow layers. However, both compaction and cementation control the evolution of porosity in the deep layers. The entire process is continuous. The trend of decreasing pores from the shallow to the deep layers is consistent. Moreover, the effect-oriented model of decreasing pores has succession and conformity (Fig. 4). Therefore, the pore volume reduction of the shallow and deep layers can be determined by the same model.

Athy (1930) proposed a model postulating that mudstone porosity is the exponential function of burial depth in normal compaction conditions. This model has been applied to the study of sandstone for a long time. However, in-depth research found that sandstone porosity is related not only to burial depth but also to geologic age (Maxwell, 1964; Schere, 1987; Hayes, 1991; Ehrenberg et al., 2009).

Liu et al. (2007) demonstrated that porosity can be expressed as the binary function of burial time and burial depth. Sandstone porosity can be computed using multiple regression analysis when burial depth and burial time are obtained. Therefore, the following decreasing pore model is established:

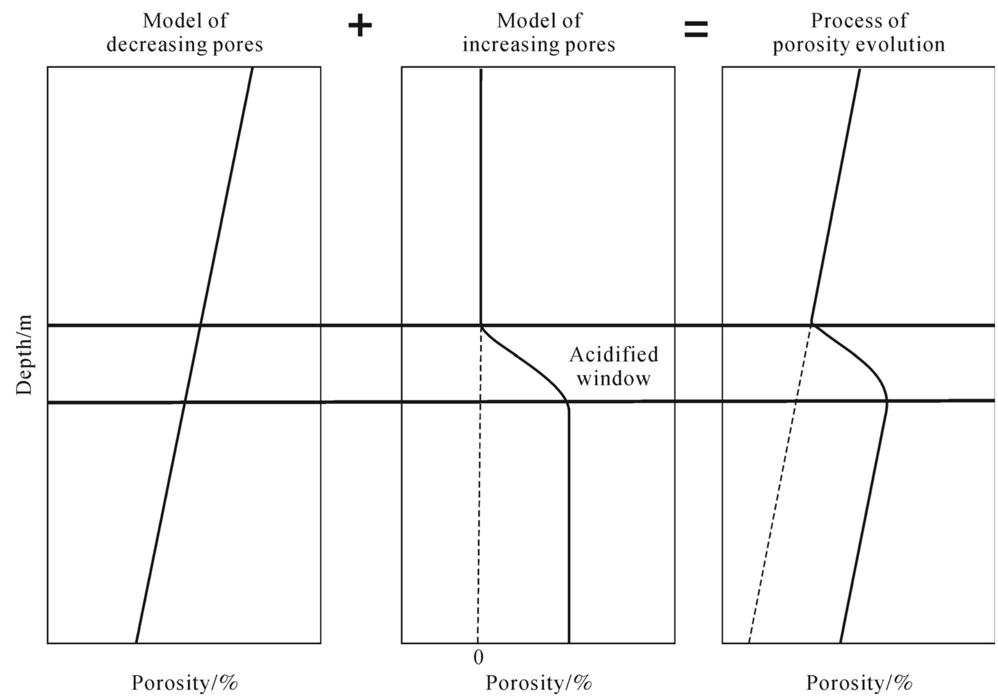

Fig. 3 The model of porosity evolution is a combination of a decreasing pores model and an increasing pores model.

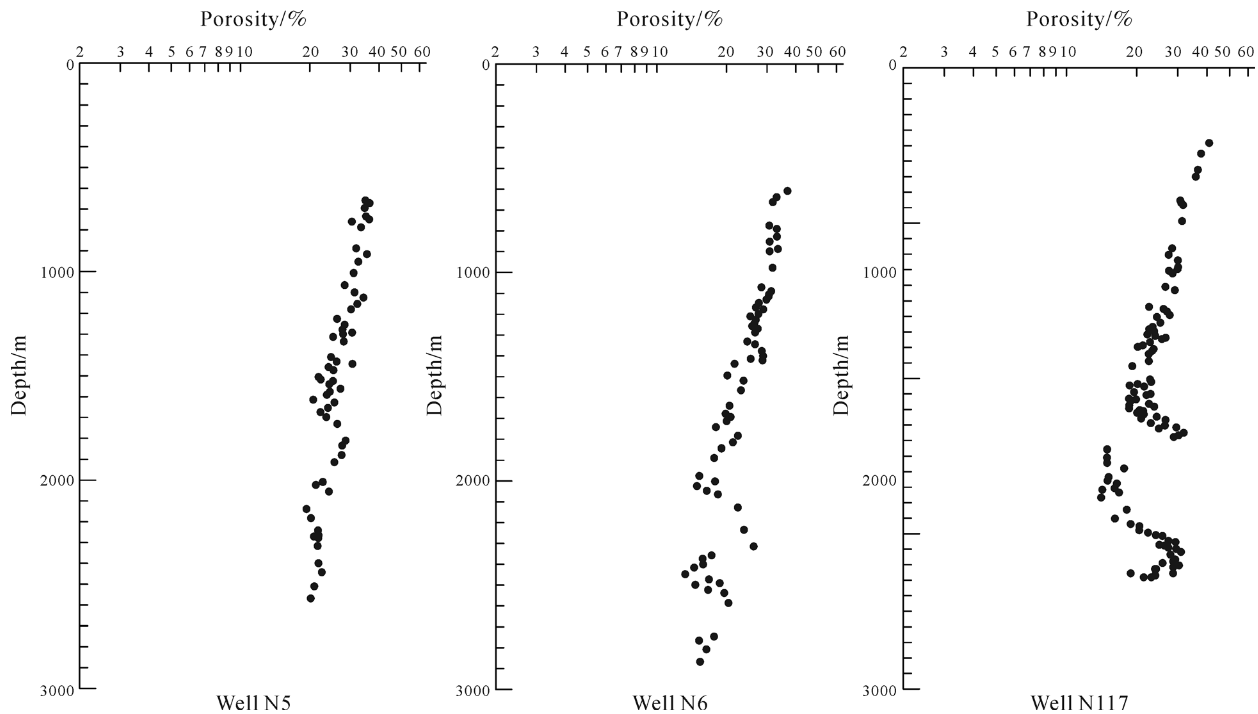

Fig. 4 Porosity sections of typical wells in the Niuzhuang Sag showing that the trend of decreasing pores is consistent between shallow layers and deep layers.

$$\phi_n = 48e^{(-0.00057z + 0.0003t + 0.00000052zt)}, \quad (1)$$

where ϕ_n is the residual porosity after compacting and cementing, %; z is burial depth, m; and t is burial time, Ma.

3.3 Increasing pore model

Corrosion generates an increase of porosity as a result of organic-acid dissolving minerals, such as carbonate and feldspar when geothermal in specific regimes (Carothers and Kharaka, 1978; Surdam et al., 1984, 1989; Schieber, 2011). With regard to the Niuzhuang Sag, Chen et al. (2009) proposed that carbonate cements are dissolved in the Jiyang subbasin when the paleotemperature is approximately 70°C. The timing of the oil charge in the Dongying Depression is inferred to be approximately 24 Ma to 20 Ma (Guo et al., 2012). Simultaneously, temperature in the Niuzhuang Sag is approximately 90°C (Fig. 5). Hydrocarbon inclusion further inhibits mineral dissolution (Johnson, 1920; Hawkins, 1978; Hayes, 1991). Thus, we define the acidified window as the period when geothermal temperatures range from 70°C to 90°C. If the temperature is below 70°C, then organic acid is insufficient to generate secondary porosity. If the temperature is over 90°C, then corrosion weakens because of the reduced concentration of organic acid and hydrocarbon emplacement.

According to the theory of chemical dynamics, reaction rate is proportional to concentration. Therefore, the dissolution rate of a mineral is proportional to the acid concentration such that

$$\frac{\partial \phi_s}{\partial t} = k_1' C + c_0', \tag{2}$$

where ϕ_s is secondary porosity caused by denudation, %; k_1' is constant of proportionality; C is concentration of the organic acid, mol/L; and c_0' is an undetermined constant.

The corresponding geothermal temperature is approximately 80°C when the concentration of organic acid in the oil field water of the Niuzhuang Sag reaches the maximum level. Therefore, we establish the relationship between organic acid concentration and geothermal temperature as follows:

$$C = a_1 T^2 + b_1 T + c_1, \tag{3}$$

where T is formation temperature, °C; and a_1, b_1, and c_1 are undetermined constants.

In a particular period, the burial depth is proportional to the burial time and geothermal temperature. Therefore, the change rate of porosity in the acidified window can be modeled as follows:

$$\frac{\partial \phi_s}{\partial t} = a' t^2 + b' t + c', \tag{4}$$

where a', b', and c' are undetermined constants.

We convert the time to geohistorical time, define the time when the geothermal temperature first reaches 70°C as t_1, and set the time when the geothermal temperature first reaches 90°C as t_2. When $t = t_1$, then $\phi_s = 0$; and when $t = t_2$, then $\phi_s = \Delta\phi$. The curve of increasing porosity is centrosymmetric. Thus, we can solve the equation above and obtain the model of secondary porosity increment in the acidified window, as follows:

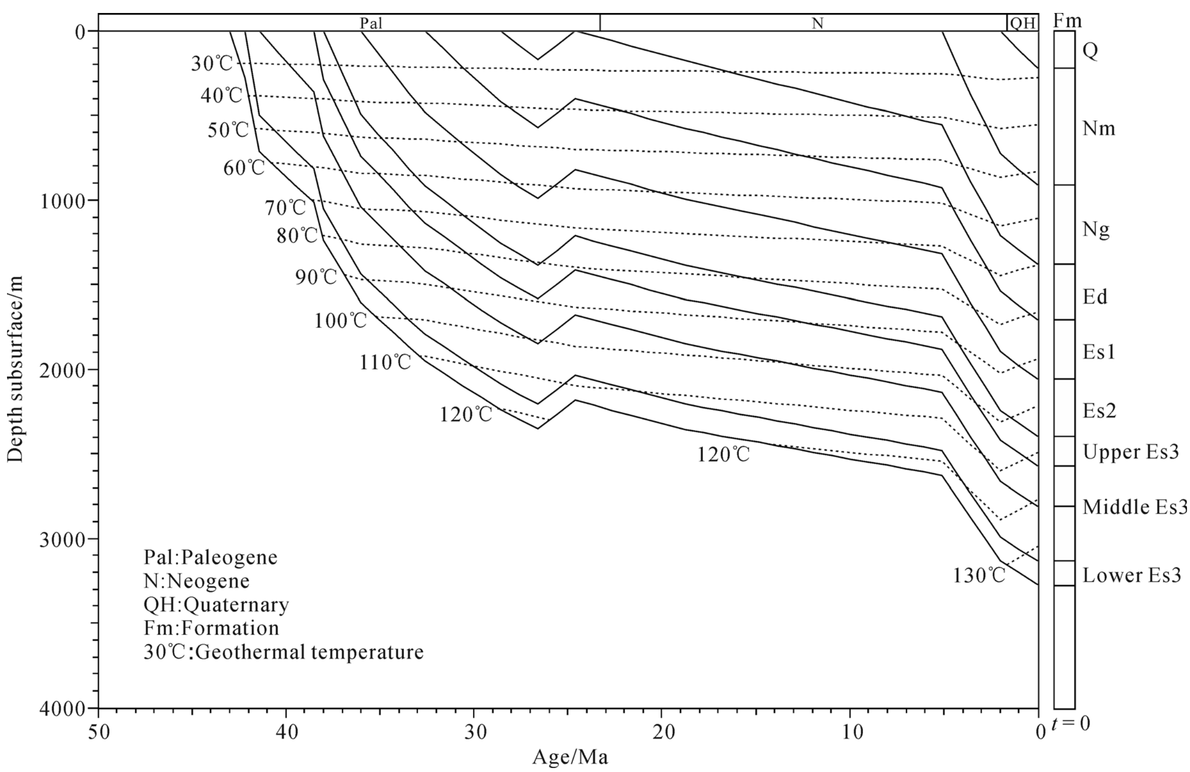

Fig. 5 The burial historian and thermal historian map of well N6 in Niuzhuang Sag showing that the temperature of the Middle Es3 member is about 90°C when the oil charging.

$$\phi_s = -\frac{2\Delta\phi}{\Delta t^3}(t-t_1)^3 + \frac{3\Delta\phi}{\Delta t^2}(t-t_1)^2, \quad (5)$$

where t is burial time, Ma; $\Delta\phi$ is actual increment of present porosity, %; t_1 is time when the geothermal temperature first reaches 70°C, Ma; t_2 is time when the geothermal temperature first reaches 90°C, Ma; Δt is time interval of the layer in the acidified window, Ma; and $\Delta t = t_2 - t_1$, Ma.

3.4 Paleoporosity recovery model

The preceding analysis shows that the process of porosity evolution can be divided into the following three stages: 1) before the layer enters the acidified window, during which no secondary pores are found, and porosity simply decreases by compaction; 2) when the layer is in the acidified window, during which pores not only increase by corrosion but also decrease by compaction and cementation; and 3) after the layer exits the acidified window, during which the porosity increment is constant and unchanging. At this stage, the layer is compacted based on secondary pores. We can then recover the paleoporosity as follows:

$$\phi = \begin{cases} \phi_0 e^{(az+bt+czt)}, t \geqslant t_1 \\ \phi_0 e^{(az+bt+czt)} - \frac{2\Delta\phi}{\Delta t^3}(t-t_1)^3 + \frac{3\Delta\phi}{\Delta t^2}(t-t_1)^2, t_1 > t > t_2, \\ \phi_0 e^{(az+bt+czt)} + \Delta\phi, t \leqslant t_2 \end{cases} \quad (6)$$

where ϕ_0 is initial porosity, %; Δt is time interval of the layer in the acidified window, Ma; $\Delta t = t_2 - t_1$; and a, b, and c are constants of the binary function.

4 Results

We take well N117 as an example. We choose the point with burial depth of 2,902 m and present porosity of 15.9% to simulate the porosity evolution with respect to time and burial depth, respectively (Fig. 6).

1) The depositing of the middle Es3 member began in 42.1 Ma. Primary porosity was 48%.

2) The strata was compressed continuously until burial depth was 1,049 m in 35.7 Ma. Meanwhile, the porosity decreased to 26.5% because of compaction.

3) The strata were in the acidified window from 35.7 Ma to 30.4 Ma, when geothermal temperature was 70°C to 90°C. Organic acid fluid eroded the minerals and formed secondary pores. Secondary porosity was 5.8% when hydrocarbon was charged in 30.4 Ma. Compaction and cementation resulted in porosity decrease by 6.2%. Therefore, actual porosity decreased by 0.4% to 26.1%.

4) The strata was compressed continuously from 30.4 Ma to 26.6 Ma until burial depth was 1,876.9 m. Meanwhile, porosity decreased to 22.7% because of compaction and cementation.

5) The strata uplifted from 26.6 Ma to 24.5 Ma. Burial depth was shallower than the previous maximum burial depth. Therefore, burial depth had no effect on porosity. However, porosity still decreased slightly by 0.1% with respect to time.

6) The strata was compressed continuously from 24.5 Ma until the present time and reaching the maximum burial depth. Compaction and cementation decreased porosity by 6.7%. At present, porosity is 15.9%.

5 Conclusions

Based on the findings, the following conclusions are obtained:

1) The proposed recovery method of sandstone paleoporosity is influenced by both destructive and constructive diagenesis. Based on simulated effects and present porosity characteristics, the evolution of porosity is decomposed into porosity decrease and porosity increase processes. Mathematical models for the evolution of these two independent processes are established. The models are time-correlated and easily employed, as well as feasible and reliable.

2) For the strata in the middle Es3 member of the Niuzhuang Sag, the Dongying Depression, and the Bohai Bay Basin, destructive diagenesis includes compaction and cementation. Constructive diagenesis is characterized by dissolution of feldspars and carbonate cements because of organic acids. The effects of compaction and cementation on the porosity include continuity and consistency between shallow and deep layers. Thus, the same model is adopted to simulate the process of decreasing total porosity. The increase of porosity occurs gradually within the acidified window of 70°C to 90°C.

3) The model of porosity decrease is a binary function of burial depth and time, which starts from sandstone sedimentation to the present. The model of porosity increase, which is mainly influenced by the paleotemperature experienced by the strata, occurs within a particular acidified window. The combination of the two models forms the evolution model of total porosity, which is a three-piecewise function corresponding to before the acidified window, within the acidified window, and after the acidified window.

4) The porosity evolution model presented in this paper is based on the sandstone in the middle Es3 member of the Niuzhuang Sag, the Dongying Depression, and the Bohai Bay Basin. However, the technique and results can be extended to different petroliferous basins.

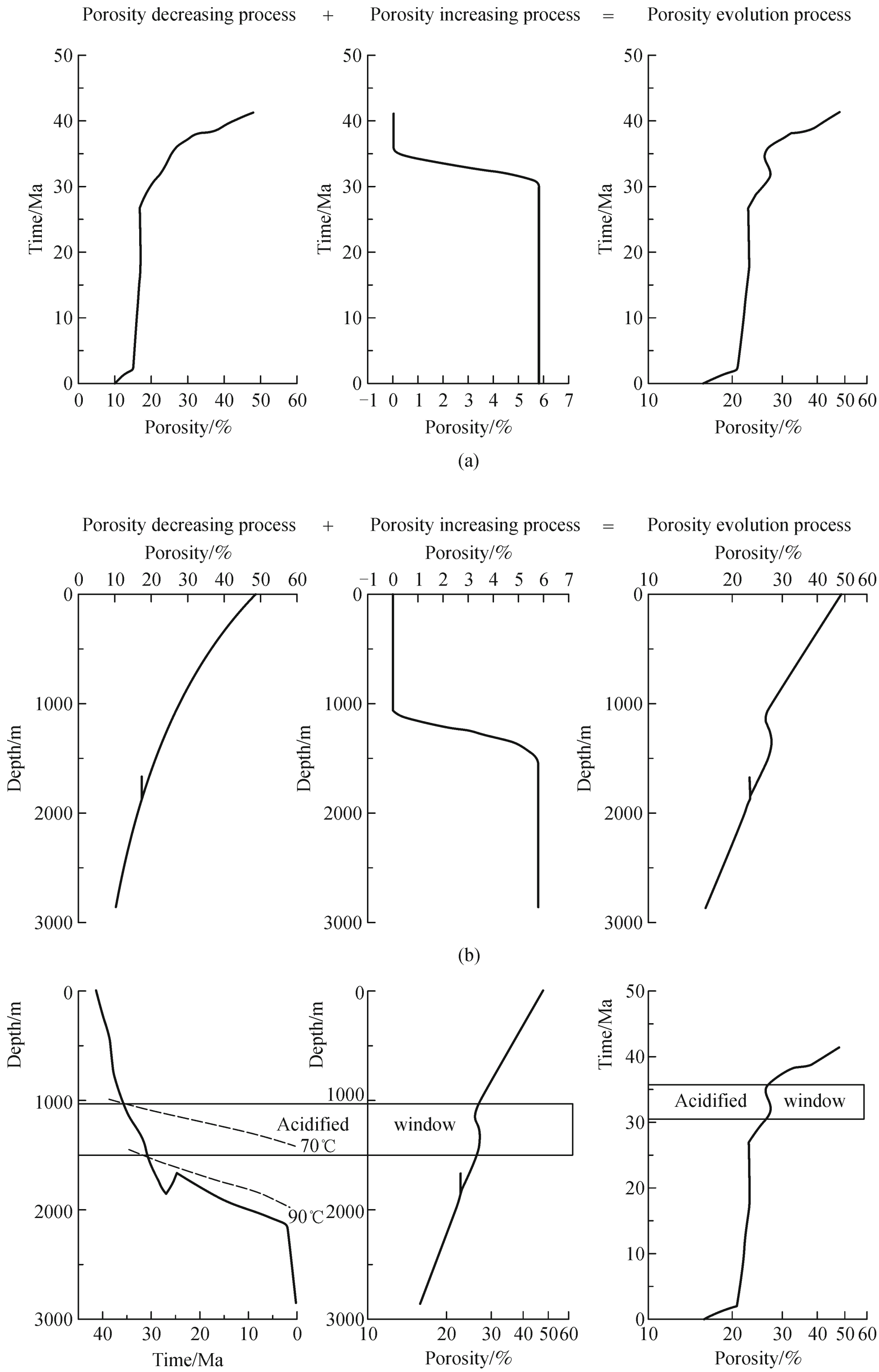

Fig. 6 The simulation of sandstone porosity evolution of well N117 from time (a), depth(b), and synthetic evolution (c) respectively.

Acknowledgements This work was supported by the Young Scholars Development Fund of SWPU (201499010089).

References

Athy L F (1930). Density, porosity and compaction of sedimentary rock. AAPG Bull, 14(1): 1–24

Bloch S, Helmold K P (1995). Approaches to predicting reservoir quality in sandstones. AAPG Bull, 79: 97–115

Bloch S, Lander R H, Bonnell L (2002). Anomalously high porosity and permeability in deeply buried sandstone reservoirs: origin and predictability. AAPG Bull, 86(2): 301–328

Bloch S, McGowen J H, Duncan J R, Brizzolara D W (1990). Porosity prediction, prior to drilling, in sandstones of the Kekiktuk Formation (Mississippian), North Slope of Alaska. AAPG Bull, 74: 1371–1385

Carothers W W, Kharaka Y K (1978). Aliphatic acid anions in oil-field waters: implications for origin of natural gas. AAPG Bull, 62(12): 2441–2453

Chen D X, Pang X Q, Jiang Z X, Zeng J H, Qiu N S, Li M W (2009). Reservoir characteristics and their effects on hydrocarbon accumulation in lacustrine turbidites in the Jiangyang Super-depression, Bohai Bay Basin, China. Mar Pet Geol, 26(2): 149–162

Deng X Q, Liu X S, Li S X (2009). The relationship between compacting history and hydrocarbon accumulating history of the super-low permeability reservoirs in the Triassic Yanchang Formation in Ordos Basin. Oil & Gas Geology, 30(2): 156–161

Dillon C G, Worden R H, Barclay S A (2004). Simulations of the effects of diagenesis on the evolution of sandstone porosity. J Sediment Res, 74(6): 877–888

Ehrenberg S N (1990). Relationship between diagenesis and reservoir quality in sandstones of the Garn Formation, Haltenbanken, mid-Norwegian continental shelf. AAPG Bull, 74(10): 1538–1558

Ehrenberg S N, Nadeau P H, Steen Ø (2009). Petroleum reservoir porosity versus depth: influence of geological age. AAPG Bull, 93 (10): 1281–1296

Gong Z S (1997). Giant Offshore Oil and Gas Fields in China. Beijing: Petroleum Industry Press, 396 (in Chinese)

Guo X W, He S, Liu K Y, Song G Q, Wang X J, Shi Z S (2010). Oil genneration as the dominant overpressure mechanism in the Cenozoic Dongying Depression, Bohai Bay Basin, China. AAPG Bull, 94(12): 1859–1881

Guo X W, Liu K Y, He S, Song G Q, Wang Y S, Hao X F, Wang B J (2012). Petroleum generration and charge history of the northern Dongying Depression, Bohai Bay Basin, China: insight from integrated fluid inclusion analysis and basin modelling. Mar Pet Geol, 32(1): 21–35

Hawkins P J (1978). Relationship between diagenesis, porosity reduction, and oil emplacement in late Carboniferous sandstone reservoirs, Bothamsall Oilfield, E Midlands. J Geol Soc London, 135 (1): 7–24

Hayes J B (1991). Porosity evolution of sandstone relates to vitrinite reflectance. Org Geochem, 17(2): 117–129

He W W, Hajash A, Sparks D (2002). A model for porosity evolution during creep compaction of sandstones. Earth Planet Sci Lett, 197(3–4): 237–244

Hu S B, O'Sullivan P B, Raza A, Kohn B P (2001). Thermal history and tectonic subsidence of the Bohai basin, northern China: a Cenozoic rifted and local pullapart basin. Phys Earth Planet Inter, 126(3–4): 221–235

Johnson R H (1920). The cementation process in sandstones. AAPG Bull, 4: 33–35

Lampe C, Song G Q, Cong L Z, Mu X (2012). Fault control on hydrocarbon migration and accumulation in the Tertiary Dongying depression, Bohai Basin, China. AAPG Bull, 96(6): 983–1000

Li M G, Zhuo X Z, Chen G, Xu T W (2009). Application of porosity evolution model to reservoir assessment of Zhuhai Formation in Enping Sag. Acta Petrol Sin, 30(6): 862–868 (in Chinese)

Li P L (2004). Oil/gas distribution patterns in Dongying Depression, Bohai Bay Basin. Journal of Petroleum cience and Engineering, 41, 57–66.

Liu Z, Shao X J, Jin B, Li H Y, Xu X M, Liang Q S (2007). Co-effect of depth and burial time on the evolution of porosity for clastic rocks during the stage of compaction. Geoscience, 21(1): 125–132 (in Chinese)

Maxwell J C (1964). Influence of depth, temperature, and geologic age on porosity of quartzose sandstone. AAPG Bull, 48(5): 697–709

Meng Y L, Wang Y C, Niu J Y, Sun H B, Yin X L, Xiao L H, Gao J J (2007). Prediction of reservoir porosity and determination of effective gas reservoirs: taking Yuanyanggou area of Bohai Bay Basin as an example. Natrual Gas Industry, 27(6): 42–44 (in Chinese with English abstract)

Pan G F, Liu Z, Zhao S, Hu Z Q, Hu X D (2011). Quantitative simulation of sandston porosity evolution: a case from Yanchang Formation of Zhenjing area, Ordos basin. Acta Petrol Sin, 32(2): 249–256 (in Chinese)

Qu D F, Jiang Z X, Liu H M, Gao Y J (2012). A reconstruction method of method of porosity for clastic reservoirs during the crucial period of hydrocarbon accumulation. Acta Petrol Sin, 33(3): 404–413 (in Chinese)

Schere M (1987). Parameters influencing porosity in sandstones: a model for sandstone porosity prediction. AAPG Bull, 71: 485–491

Schieber J (2011). Marcasite black shale-a mineral proxy for oxygenated bottom waters and intermittent oxidation of carbonaceous muds. J Sediment Res, 81(7): 447–458

Surdam R C, Boese S W, Crossey L J (1984). The chemistry of secondary porosity. AAPG Mem, 37: 127–149

Surdam R C, Crossey L J, Hangen E S, Heasler H P (1989). Organic-inorganic interactions and sandstone diagenesis. AAPG Bull, 73(1): 1–23

Wang R F, Shen P P, Zhao J L (2011). Diagenesis of deep sandstone reservoirs and a quantitative model of porosity evolution: taking the third member of Shahejie Formation in the Wendong Oilfield, Dongpu Sag, as an example. Petroleum Exploration and Development, 38(5): 552–559

Wangen M (1998). Modeling porosity evolution and cementation of sandstones. Mar Pet Geol, 15(5): 453–465

Yang R C, Fan A P, Han Z Z, Wang X P (2012). Diagenesis and porosity evolution of sandstone reservoirs in the East II part of Sulige gas field, Ordos Basin. International Journal of Mining Science and Technology, 22(3): 311–316

Zhang L Y, Liu Q, Zhu R F, Li Z, Lu X C (2009). Source rocks in

Mesozoic-Cenozoic continental rift basins, East China: a case from Dongying Depression, Bohai Bay Basin. Org Geochem, 40(2): 229–242

Zhang S W, Wang Y S, Shi D S, Xu H M, Pang X Q, Li M W (2004). Fault-fracture mesh petroleum plays in the Jiyang Superdepression of the Bohai Bay Basin, eastern China. Mar Pet Geol, 21(6): 651–668

Zhu B J, Cheng H H, Qiao Y C, Liu C, Shi Y L, Zhang K, Sun D S, Lin W R (2012). Porosity and permeability evolution and evolution in anisotropic porosity multiscale-multiphase-multicomponent structure. Chin Sci Bull, 57(4): 320–327